Soils and Rocks

An International Journal of Geotechnical and Geoenvironmental Engineering

www.soilsandrocks.com

ISSN 1980-9743
ISSN-e 2675-5475

Relationship between Point Load Strength Index and Slake Durability Index of sandstones from the Amile Formation, Tansen Group, West-Central Nepal

Article

Saurav Poudel[1], Naresh Kazi Tamrakar[1#]

Keywords
Slake Durability Index
Point Load Strength Index
Quartzose sandstones
Amile Formation
Correlation

Abstract

Point load strength index (*PLSI*) and slake durability index (*SDI*) are two important indices of rocks used to evaluate strength and durability for various engineering applications. This research investigates these two indices in sandstones from the Amile formation coupled with petrography, aiming to determine the strength and durability of rock, and test for correlations among mineral constituents, texture, *PLSI*, and *SDI* to develop empirical relationships among them. The study provides insights into the geotechnical properties of an important geological formation in the Lesser Himalayan Zone, contributing valuable data for infrastructure development. The methodology involved field sampling, petrographic analysis of thin sections, *SDI* testing over two cycles, and *PLSI t*esting on irregular lump samples. Correlations between *SDI*, *PLSI*, water absorption, packing density, and packing proximity were statistically analyzed. Quarztose sandstones have extremely high durability (*SDI*: 99.17–99.78%), very strong to extremely strong compressive strength (*PLSI*: 5.94–14.81 MPa), and low water absorption values (*WAV*: 0–2.17%). Very high positive correlations were found between *SDI* and *PLSI* with R^2 =0.804. Based on this correlation, future research can use the equation *SDI* = 0.0712*PLSI* + 98.727 to estimate durability from strength for similar sandstones, saving time and resources.

1. Introduction

Rock strength and durability evaluation is critical for assessing geological materials in engineering applications (Hatheway, 2009). Index tests like the Point Load Strength Index (*PLSI*) and Slake Durability Index (*SDI*) offer efficient methods for characterizing rock mechanical properties (Bieniawski, 1975; ISRM, 1985). These tests are valuable for determining construction material quality and predicting rock mass behavior under various conditions (Gokceoglu et al., 2000; Tamrakar et al., 2007).

PLSI provides a simple estimate of rock strength, correlating with uniaxial compressive strength (*UCS*) while requiring less sample preparation (Broch & Franklin, 1972). *SDI* evaluates rock resistance to weathering through repeated wetting and drying cycles (Franklin & Chandra, 1972; Gamble, 1971).

Previous studies on sandstones in Nepal have reported varying *PLSI* and *SDI* values. For instance, (Sharma & Tamrakar, 2023) found *PLSI* values ranging from 2.40 to 11.4 MPa for the Fagfog Quartzite, while (Budhathoki & Tamrakar, 2022) reported *PLSI* and *SDI* values ranging from 0.024 to 2.16 MPa and 93.23% to 30.37% respectively for sandstones in the Siwalik Group. Sandstones from the Sneinton Formation in England are moderately strong and deformable and durability correlates with quartz content and clay fraction (Bell & Culshaw, 1998). Sabatakakis et al., (2008) reported *PLSI* values for sandstones ranging from 0.5 to 5.7 MPa. Tsiambaos & Sabatakakis (2004) found that the *PLSI* of sandstones varied between 0.5 and 8.4 MPa, correlating strongly with *UCS*. Dhakal et al. (2002) reported *SDI* values for sandstones ranging from 90% to 99% after two cycles, emphasizing the role of mineralogy in durability characteristics. Celik & Kacmaz (2016) observed *SDI* values for various building stones, including sandstones, ranging from 94.8% to 99.6%. demonstrating their high resistance to weathering. Shakoor & Bonelli (1991) found *SDI* values for sandstones between 86% and 100%, correlating with petrographic characteristics and other engineering properties.

The Water Absorption Test, measuring rocks' water absorption, provides insights into porosity, permeability, and degradation susceptibility (ASTM, 2019; Benavente et al.,

Naresh Kazi Tamrakar[1] E-mail address: naresh.tamrakar@cdgl.tu.edu.np
[1]Tribhuvan University Kirtipur, Central Department of Geology, Kathmandu, Nepal.

Submitted on August 24, 2024; Final Acceptance on January 13, 2025; Discussion open until August 31, 2025.

Editor: Renato P. Cunha

https://doi.org/10.28927/SR.2025.006924

2015). Sandstone water absorption values typically range from less than 1% to over 20% (Bell, 2007; Celik & Kacmaz, 2016).

Multivariate correlation is a statistical technique used to analyze relationships among variables by considering three or more variables at once. In the context of rock mechanics, multivariate analysis can reveal how different petrographic, physical, and mechanical properties interrelate, providing insights that may not be apparent from simple bivariate correlations (Shakoor & Bonelli, 1991). For instance, studies by Bell & Lindsay (1999) and Tamrakar et al. (2007) have used multivariate techniques to investigate the influence of petrographic properties. In this research, multivariate correlation is used to explore how petrographic properties along with water absorption relate with *PLSI* and *SDI* of sandstone samples.

The Amile Formation, part of the Tansen Group in west-central Nepal, is distributed well in the hillslopes of the Siddhartha Highway (Figure 1). Understanding the strength and durability characteristics of sandstone is crucial for assessing their suitability as construction materials and comprehending geological factors influencing slope stability. This research aims to determine the *PLSI*, *SDI,* packing density, packing proximity, and water absorption values of sandstones from the Amile Formation, and explore correlations between them.

2. Geological setting of the study area

The Tansen Area is located within the Lesser Himalayan Zone of west-central Nepal. This zone lies between the Main Boundary Thrust (MBT) to the south and the Main Central Thrust (MCT*)* to the north. The Lesser Himalayan rocks in this region consist of low-grade metasedimentary sequences (Sakai, 1983). The Precambrian rocks in the Tansen Area belong to the Kali Gandaki Supergroup. The younger sedimentary sequence is represented by the Tansen Group, comprising the Dumri Formation, Bhainskate Formation, Amile Formation, Taltung Formation, and the Sisne Formation (Figure 2). The Lesser Himalayan rocks in the Tansen Area exhibit typical structural features like thrusts, folds, and the emplacement of the Lesser Himalayan nappes.

A huge syncline exists in the study area, where the younger sequence of the Tansen Group of rocks is overlain by the older Heklang Formation and the Virkot Quartzite of the Kali Gandaki Supergroup with tectonic contacts. The formations of the Kali Gandaki Supergroup were brought as tectonic clippe. The study area particularly lies in the northern limb of the syncline.

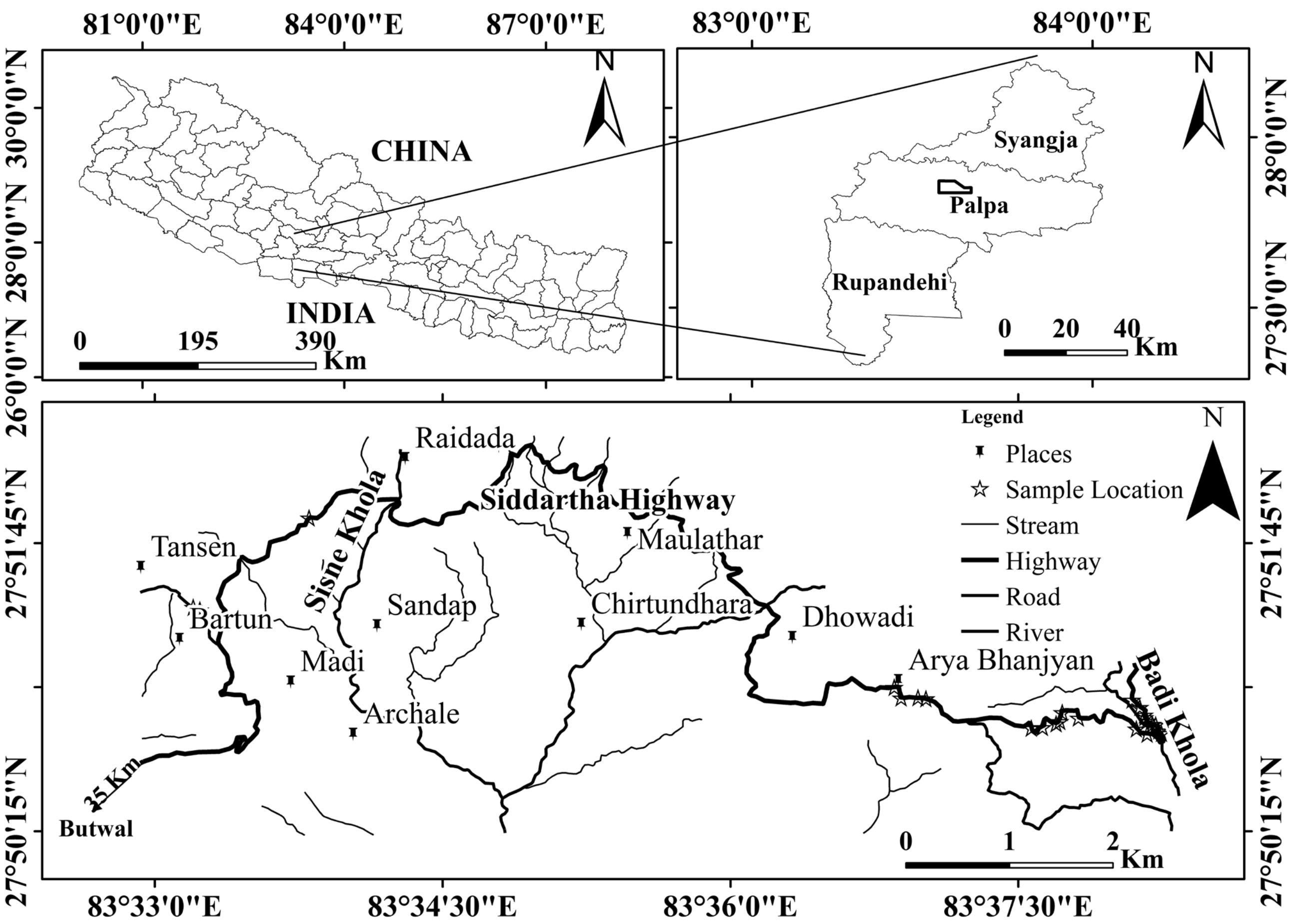

Figure 1. Location map showing study area.

3. Methodology

3.1 Sampling

Twenty-five sampling locations (Figure 2) were selected across the study area. From each location, ten fresh sandstone fragments (40-60g each) were collected for *SDI* testing, and three orthorhombic samples were taken for *PLSI* determination.

3.2 Microscopic examination of sandstone

Thin sections were examined under a polarizing light microscope to analyze rock composition, texture, packing density, packing proximity, and grain characteristics (size, sorting, roundness, and interlocking fabrics). Packing density (*Pd*) and Packing proximity (*Pp*) were measured using the expressions of Kahn (1956):

$$Pd = \{(11+12+13.....+ln)/L\}.100(\%) \quad (1)$$

$$Pp = \{(gl+g2+g3+.....gn/Nc\}.100(\%) \quad (2)$$

where: ln = length of grains across the traverse line and L is the traverse length, and Gn = grain-to-grain contact and Nc is the total number of contacts.

3.3 Testing for Point Load Strength Index

A point Load Test of irregular lumps ranging in thickness of 25-30 mm was performed following ASTM D5731 02 (ASTM, 2003). The point load strength index $I_{s(50)}$ is calculated using:

$$I_{s(50)} = F \times Is \quad (3)$$

where: $I_{s(50)}$ = corrected point load strength; F= Size correction factor; and I_s= Uncorrected Point load strength index, MPa.

$I_{s(50)}$ was used to calculate the *UCS* of the test sample using an empirical relation (Vallejo et al., 1989).

$$UCS = 17.4 \times I_{s(50)} \quad (4)$$

The value obtained for the *UCS* of the test sample was employed to classify the rock with the reference of ISRM (1981) (Table 1).

3.4 Testing for SDI following ASTM D4644-87

To conduct the test, the ASTM procedure D4644 standard procedure is used. For determining the sandstone's durability, the standard cycle i.e., the second cycle (I_{d2}) of the Slake Durability Index was compared to the classification proposed by Franklin & Chandra (1972) (Table 2).The I_{d2} is obtained from:

$$Id2 = WF / B \quad (5)$$

Table 1. Uniaxial compressive strength index classification (ISRM, 1981).

UCS (MPa)	Strength Classification
0.25 – 1	Extremely Weak
1 – 5	Very Weak
5 – 25	Weak
25 – 50	Medium Strong
50 – 100	Strong
100 – 250	Very Strong
>250	Extremely Strong

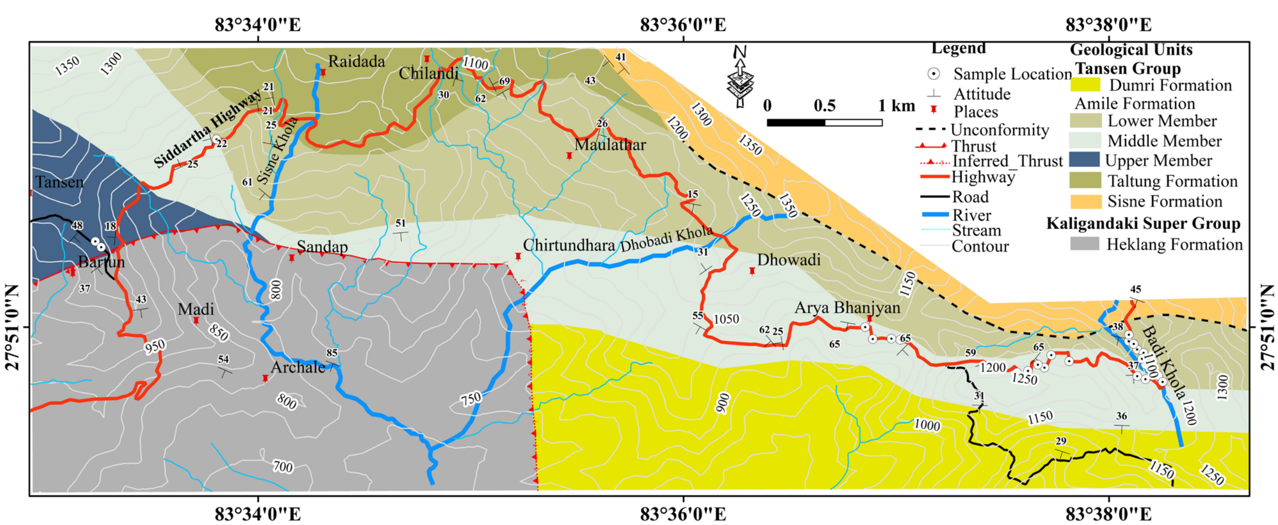

Figure 2. Geological map of study area.

where: I_{d2} = slake durability index (second cycle); WF = mass of oven-dried sample retained after the second cycle, gm; and B = mass of the oven-dried sample before the second cycle, gm.

3.5 Testing for Water Absorption test following ASTM C127

For conducting the test, standard procedure ASTM C127 (ASTM, 2011) was used. The water absorption is calculated using the formula:

$$WAV = \left(\left(B - A\right) / A\right) * 100 \tag{6}$$

where: WAV = Water Absorption Value; A =Mass of oven-dried sample; and B = Mass of saturated sample.

3.6 Linear regression correlation

Linear regression is a statistical method that analyzes relationships between continuous variables, fitting a linear equation to observed data for predictions and insights. This study uses linear regression to explore the correlation between strength, durability, and factors like water absorption, packing density, and packing proximity.

3.7 Multivariate correlation

Multivariate correlation analyzes relationships among multiple variables simultaneously extending beyond simple bivariate correlations. This study used multivariate correlation to examine relationships between *SDI, PLSI, WAV, Pd*, and *Pp*. The analysis, conducted in two phases with *SDI* and *PLSI* as dependent variables, assessed how various properties collectively influence rock durability and strength, providing a comprehensive understanding of complex interactions among studied rock properties.

4 Results

4.1 Lithological description of Quartose Sandstone in sampling sites

The exposure consists of thick-bedded (40 cm) coarse-grained, moderately weathered, pebble-bearing sandstone with ferruginous molting having pebbles of diameter 3-4 cm interbedded with thick-bedded purple shale. Thin to medium bedded, coarse-grained grey quartose sandstone interbedded with medium bedded, moderately weathered muddy sandstone. Thick-bedded coarse-grained quartzose sandstone with hematite and siderite speckles interbedded with reddish-brown siltstone. Medium bedded (10-20 cm) moderately weathered grey fresh siltstone with pisolites and thin-bedded fine-grained dark grey moderately weathered limestone. Thick-bedded coarse-grained white quartzose sandstone interbedded with medium to thick-bedded muddy sandstone, bioturbated muddy sandstone, and carbonaceous shale.

Table 2. Slake durability index classification (after Franklin & Chandra, 1972).

I_{d2} (%)	Durability Classification
0-25	Very Low
26-50	Low
51-75	Medium
76-90	High
91-95	Very High
96-100	Extremely High

4.2 Description of rock thin sections under Polarizing Microscope

The composition and texture of each sample were determined through meticulous petrographic examination, to understand their potential influence on slaking behavior and rock strength. Thin sections were analyzed under cross-polarized light (XPL) conditions (Figure 3). Figure 3 consists of six different samples: LA1(a) exhibits a poorly sorted Quartz Wacke with the (94.69% quartz, 5.31% feldspar, 16% matrix); LA9(b), a moderately sorted Subarkose arenite with (94.83% quartz, 5.17% feldspar, 3% matrix); MA1(c), Subarkose arenite with lower quartz content and insignificant mica presence than LA9(b) (94.36% quartz, 1.88% rock fragments, 0.36% mica); MA7(d), a poorly sorted Lithic Wacke with a significantly lower matrix percentage them LA1(a) and the third highest percentage of rock fragments in the plate (87.04% quartz, 8.17% rock fragments, 15.37% matrix); UA1(e), a well- sorted Quartz arenite (95.5% quartz, 4.5% feldspar); UA2(f), Quartz arenite with the highest quartz content among the samples with (98.73% quartz, 1.27% feldspar). The detailed compositional result along with the microscopically observable texture of rocks, subsequent rock classification, *Pd* and *Pp* is tabulated below (Table 3 and Table 4).

4.3 Point-load strength index (*PLSI*)

The obtained strength index values are presented in a table, where samples from the Lower Middle and the Upper Members are indicated by LA, MA, and UA, respectively. Sample LA10 exhibited the highest strength of 14.81 MPa among all the samples tested (Table 5). In contrast, sample MA9 had the lowest durability with a strength value of 5.94 MPa. According to the calculated value of *UCS* (Vallejo et al., 1989), the test samples are classified as extremely strong to very strong rock based on Brown (1981), (Table 4).

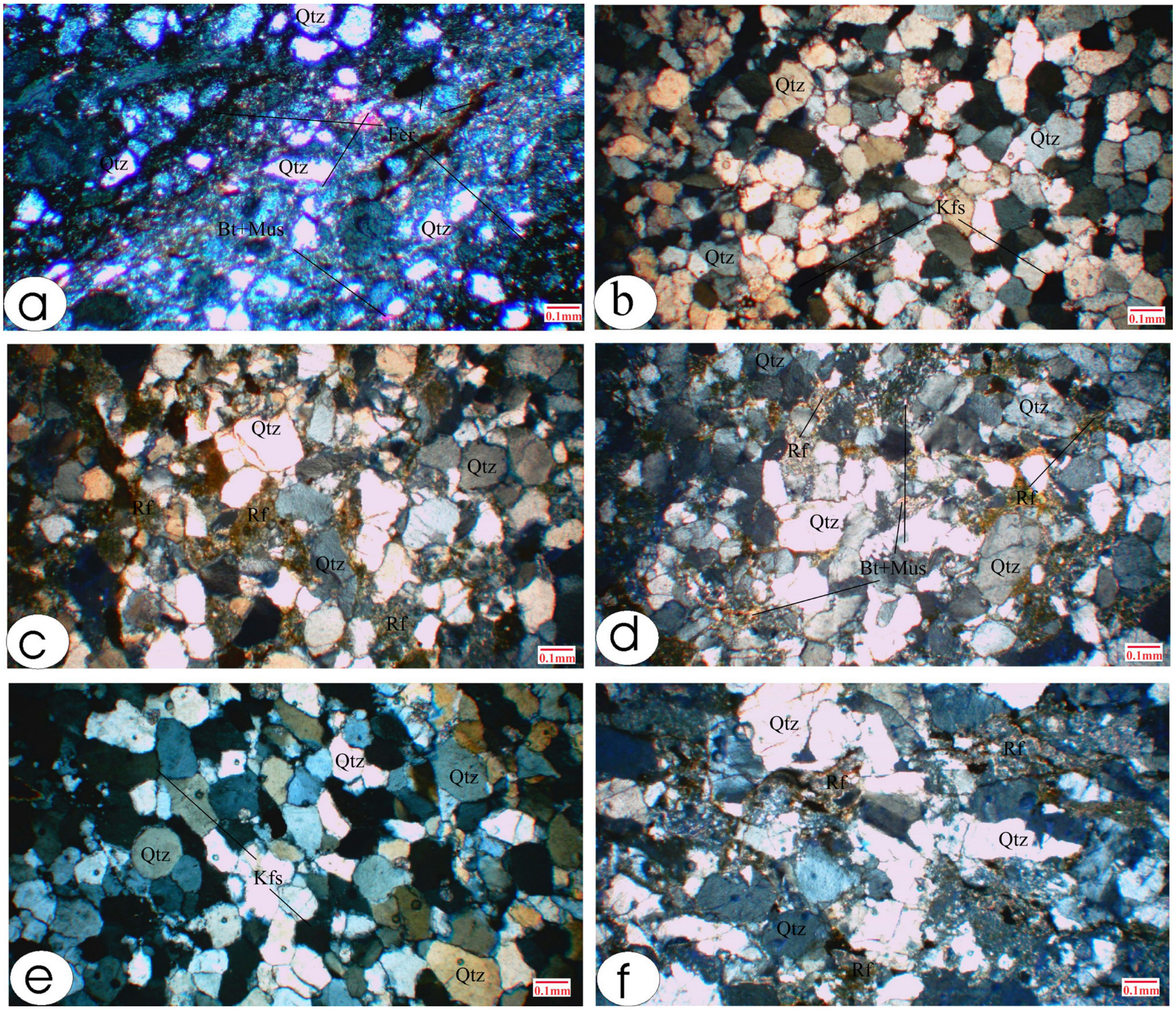

Figure 3. Photomicrograph of Sandstone from The Amile Formation under XPL sample LA1 (a) LA9 (b) MA1 (c) MA7 (d) UA1 (e) and UA2 (f).

4.4 Slake Durability Index (*SDI*)

As per the value of *SDI* of the second cycle, the value ranged from 99.78% (MA1) to 99.17% (LA2, MA5). The test sample lies on the type I disintegration pattern, ASTM D464487 (ASTM, 2001) Method. According to the classification proposed by Franklin & Chandra (1972), these values correspond to an extremely high durability rating (Table 6).

4.5 Water absorption test

The *WAV* ranges from 0 to 2.17% (MA9). According to the ASTM (2011) C 127 specification, the sample > 3% *WAV* indicates a high effective porosity whereas below 3% indicates a low effect of porosity which is seen in all samples (Table 7).

4.6 Linear regression correlation

The study examined the relationship between *SDI* and *PLSI* by plotting them on a scatter chart and calculating the best-fit line with a 95% confidence level and the relationship coefficient (R^2) (Figure 4). The analysis showed a strong correlation between *SDI* and *PLSI* across all samples, with a coefficient of determination (R^2 = 0.804), significantly higher than the critical R-value of 0.337, indicating statistical significance.

A good correlation was found between *PLSI* vs *WAV* (R^2 = 0.79), *PLSI* vs *Pd* (R^2= 0.88), *PLSI* vs *Pp* (R^2= 0.83), *SDI* vs *WAV* (R^2= 0.74), *SDI* vs *Pd* (R^2= 0.84) and *SDI* vs *Pp* (R^2= 0.78). All these correlations were statistically significant, reinforcing the connection between these indices and the measured properties (Table 8)

Table 3. Result of the petrographic analysis of sandstone from the Amile Formation.

SN	Clast (%)						Matrix (%)	Cement (%)			Packing density (Pd%)	Packing Proximity (P_p %)
	Quartz		*F*	*RF*	Mica	Others+ Heavies		Ferr.	Sil.	Arg.		
	Qm	*Qp*										
LA1	44.57	8.88	3		2	2.59	16	10		12.96	97.7	92.2
LA2	67.7	10.12	1.18			1.00	3		11	6.00	87.2	82.4
LA3	63.92	5.08	5			1.00	3	6	12	4.00	97.0	93.2
LA4	68.7	4.96	1.49			1.85	2	6	9	6.00	95.2	90.3
LA5	73.64	2.32	1.09			1.41	3	8	6	4.54	94.4	89.9
LA6	75.88	2.12	2			1.00	2	11	6		94.5	88.3
LA7	46.36	9.36	3		2	1.86	16	9		12.42	93.7	88.7
LA8	73.22	4.63	1.39			1.4.	3	5	7	4.36	94.9	89.4
LA9	72.73	2.36	4.09			2.00	3	5	7	3.82	93.4	88.7
LA10	69.77	5.12	5.75			1.03		4.15	9	5.18	97.4	91.7
MA1	65.61	9.73	3	1.50	0.36	1.95	7.09	6.76	2	2.00	97.8	90.2
MA2	64.73	2.21	3.47	7.31	0.58	1.00	9.01	5.69	3	3.00	87.0	82.6
MA3	63.09	2.31	5.01	6.00		1.27	14	1.32	2	5.00	87.4	81.5
MA4	58.61	3.49	6.04	5.52		1.05	16	2.29	4	3.00	97.8	91.3
MA5	65.83	2.19	4.21	6.57		1.77	10	2.43	3	4.00	87.4	82.7
MA6	66.43	2.71	3.49	6.69		1.32	12	2.36	2	3.00	88.1	83.0
MA7	61.01	4.83	3.62	6.18	1	1.59	15.37	0.93	1	4.47	93.3	89.0
MA8	56.53	1	6.02	8.00	1	1.38	18	2.38	1	4.69	89.7	83.6
MA9	59.84	1.09	4.74	6.00	1	1.00	15	4.52	2	4.00	87.1	82.6
MA10	64.46	2.18	1.04	8.00	1	1.29	15	1.00	2	4.03	97.4	92.7
MA11	52.65	4.89	2	12.00		1.50	17	3.00	3	3.96	93.2	88.6
MA12	50.98	3.80	3	12.00		1.00	19	4.00	2	4.22	96.1	91.8
MA13	65.54	2.32	2.19	7.00		1.08	13	3.00	2	3.87	87.1	83.7
UA1	82.63		3.89			1.61	1	3.00	6	1.87	97.0	91.5
UA2	82.43	1	1.07			1.64	1	3.00	8	1.86	97.7	91.8

4.7 Multivariant correlation

To create a more accurate predictive model with a higher R^2, we conducted multiple regression analyses for each property. Each analysis used one test as the dependent variable and the other four as independent variables. We identified significant independent variables based on their P-values, discarding those that were insignificant.

For the prediction of *PLSI*, our analysis revealed that *SDI*, *WAV*, and *Pd* were the most significant independent variables. While single regression analysis showed *Pd* as the best predictor for *PLSI* with an R^2 of 0.88, combining the three significant independent variables in a multiple regression model improved the correlation strength, resulting in an R^2 of 0.916. This R^2 value remained unchanged when only *WAV* and *Pd* were kept as independent variables (Table 9).

In the case of *SDI* prediction, *WAV* and *Pd* emerged as the most significant independent variables. The initial correlation between *SDI* and *Pd* yielded an R^2 of 0.845. To enhance the reliability of the prediction, we performed multiple regression, which slightly increased the R^2 to 0.869. Interestingly, this R^2 value remained unchanged when *PLSI* and *WAV* were included alongside *Pd* as independent variables.

5. Discussion

SDI values for sandstone from the Amile Formation ranged from 99.17% to 99.78% after the second cycle, indicating extremely high durability (Franklin & Chandra, 1972). This range is comparable to high/very high *SDI* values reported for quartzite from the Fagfog Quartzite (Sharma & Tamrakar, 2023), but higher than sandstone from the Siwalik Sub-group (30.37%-93.23%) from Hetauda (Budhathoki & Tamrakar, 2022). Spherical samples generally yielded higher index values than irregular samples (Cicek et al., 2016). The results are similar to, but slightly better than, those sandstone from an underground coal mine at the United Mineral Coal Company Sor-range (97.36%-98.71%) at 4000 ft depth (Ahmed et al., 2022).

Analysis of results showed sample MA1 had the highest *SDI* and LA2 the lowest. This correlates directly with quartz content, where MA1 had high quartz content and LA2 low, consistent with findings from Bell & Culshaw (1998) for sandstone from the Sneinton Formation. All samples exhibited a Type I disintegration pattern after the second cycle.

PLSI values for sandstone from the Amile Formation ranged from 5.94 MPa to 14.81 MPa, higher than those reported

Table 4. Texture and classification of sandstone from the Amile Formation.

SN	Texture				Recalculation (%)			Type
	Size (μm)		Shape	Sorting				
	Range	Model			*Q*	*F*	*RF*	
LA1	50-130	200	Angular	Poorly Sorted	94.69	5.31	0	Quartz wacke
LA2	40-110	180	Sub Angular	Poorly Sorted	98.51	1.49	0	Quartz arenite
LA3	60-140	210	Sub Angular	Moderate	93.24	6.76	0	Subarkose arenite
LA4	70-130	190	Sub Angular	Moderate	98.02	1.98	0	Quartz arenite
LA5	60-130	220	Sub Angular	Moderate	98.59	1.41	0	Quartz arenite
LA6	50-200	280	Sub Angular	Moderate	97.5	2.50	0	Quartz arenite
LA7	40-120	190	Angular	Poorly Sorted	94.89	5.11	0	Quartz wacke
LA8	50-150	230	Sub Angular	Moderate	98.25	1.75	0	Quartz arenite
LA9	50-140	150	Sub Angular	Moderate	94.83	5.17	0	Subarkose arenite
LA10	100-500	600	Sub Angular	Moderate	92.87	7.13	0	Subarkose arenite
MA1	50-220	400	Sub Angular	Moderate	94.36	3.76	1.88	Subarkose arenite
MA2	40-200	260	Sub Angular	Moderate	86.13	4.46	9.41	Sublitharenite
MA3	30-170	200	Sub Angular	Moderate	85.59	6.56	7.85	Sublitharenite
MA4	50-150	300	Angular	Poorly sorted	84.31	8.20	7.49	Feldspathic wacke
MA5	40-130	280	Sub Angular	Moderate	86.32	5.34	8.34	Sublitharenite
MA6	40-140	290	Sub Angular	Moderate	87.17	4.40	8.43	Sublitharenite
MA7	60-250	300	Angular	Poorly sorted	87.04	4.79	8.17	Lithic wacke
MA8	40-110	150	Angular	Poorly sorted	80.41	8.41	11.18	Lithic wacke
MA9	40-230	300	Sub Angular	Moderate	85.01	6.61	8.37	Sublitharenite
MA10	50-200	300	Sub Angular	Moderate	88.05	1.37	10.57	Sublitharenite
MA11	40-210	260	Angular	Poorly sorted	80.43	2.80	16.77	Lithic wacke
MA12	30-200	600	Sub Angular	Moderate	78.50	4.30	17.2	Lithic wacke
MA13	50-180	240	Sub Angular	Moderate	88.07	2.84	9.09	Sublitharenite
UA1	60-220	320	Rounded	Well sorted	95.50	4.50	0	Quartz arenite
UA2	130-520	700	Rounded	Well sorted	98.73	1.27	0	Quartz arenite

for quartzite from the Fagfog Quartzite (2.40-11.4 MPa) by (Sharma & Tamrakar, 2023) and sandstone from the Siwalik Sub-group (0.024-2.16 MPa) by (Budhathoki & Tamrakar, 2022). Based on calculated *UCS* values, samples are classified as extremely strong to very strong (Brown, 1981). Lower *PLSI* values may be influenced by smaller sample sizes. Higher quartz content correlates with higher *UCS* (Sabatakakis et al., 2008), while feldspar can reduce strength (Yusof & Zabidi, 2016). Lower moisture content is associated with higher strength (Aligholi et al., 2017), as observed in samples LA3, LA6, LA10, MA9, and MA11. Samples with higher moisture content (LA9, MA1, MA4, MA6, MA7) showed lower *PLSI* values. Mica presence can reduce rock strength (Yasir et al., 2018), consistent with observations in samples LA1, MA1, MA2, MA7, and MA10. The highest *PLSI* value (sample LA10) corresponded to a lack of mica.

The samples LA1, LA10, UA1, and LA2 have higher *SDI* values and are found predominantly of quartz whereas samples MA2, MA5, MA7, and MA9 have relatively low *SDI* values and are found less quartz content. The sample having a higher *SDI* value has the least amount of matrix whereas the sample having a lower value of *SDI* has more than 15% matrix. Discontinuous matrix sandstones exhibit lower durability than those with continuous matrices (Tugrul & Zarif 1998). The present study found that samples having matrix, rock fragments, and mica may have slightly lower durability. Sandstone rich in smectite and zeolite had higher durability than pyroclastic rocks with just smectite (Dhakal et al., 2002).

Yusof & Zabidi (2016) found that the rock containing a high percentage of quartz gave high strength in this context, the sample UA1 and UA2 with maximum strength is found to have high quartz content whereas samples MA2, MA9, and MA13 with minimum strength is found to have less quartz content. There were no strong correlations between point load and slake durability with mineralogy (Ayakwah et al., 2009).

WAV for sandstone from the Amile Formation ranged from 0% to 2.17%, indicating low effective porosity (below 3%) according to ASTM C 128 specifications. These values are comparable to the low water absorption values reported for quartzite from the Fagfog Quartzite in Nepal (Sharma & Tamrakar, 2023) but lower than sandstone from the Siwalik Sub-groups (1.26% to 17.6%) in Hetauda (Budhathoki & Tamrakar, 2022). Samples with high quartz content showed 0% *WAV*. The low *WAV* indicates high durability and weathering resistance, similar to sandstone from the Sneinton Formation in England (0.3% to 2.5%) reported by Bell & Culshaw (1998), which correlated with high durability and strength.

Table 5. Point load strength index values of sandstones from the Amile Formation.

SN	Thickness avg(mm)	Width avg (mm)	Load (*kN*)	*De* (mm)	*De*^{2} (mm^2)	I_S (MPa)	*F* (mm)	$I_{s(50)}$ (MPa)	*UCS* (MPa)	Class
LA1	29.5	53.4	26.78	44.79	2005.73	13.35	0.95	12.71	221.09	V. strong
LA2	25.5	44.7	11.58	38.10	1451.30	7.98	0.88	7.06	122.85	V. strong
LA3	28.3	47.5	25.22	41.37	1711.55	14.74	0.92	13.53	235.44	V. strong
LA4	26.7	43.8	18.14	38.59	1489.00	12.18	0.89	10.84	188.65	V. strong
LA5	26.5	47.3	18.93	39.95	1595.94	11.86	0.90	10.72	186.56	V. strong
LA6	27.6	48.2	20.42	41.16	1693.82	12.06	0.92	11.04	192.18	V. strong
LA7	26.8	47.5	18.81	40.26	1620.83	11.61	0.91	10.53	183.17	V. strong
LA8	26.2	46.7	18.64	39.47	1557.86	11.97	0.90	10.76	187.18	V. strong
LA9	27.4	45.45	17.34	39.82	1585.60	10.94	0.90	9.87	171.76	V. strong
LA10	27.8	44.7	25.97	39.78	1582.20	16.41	0.90	14.81	257.67	E. strong
MA1	28.3	45.35	22.28	40.42	1634.08	13.63	0.91	12.39	215.60	V. strong
MA2	28.7	48.8	12.3	42.23	1783.25	6.90	0.93	6.39	111.23	V. strong
MA3	26.7	54.1	16.64	42.89	1839.16	9.05	0.93	8.44	146.92	V. strong
MA4	28.5	48.4	24.76	41.91	1756.31	14.10	0.92	13.02	226.57	V. strong
MA5	25.7	45.5	11.92	38.59	1488.86	8.01	0.89	7.12	123.97	V. strong
MA6	28.8	45.8	16.5	40.98	1679.45	9.82	0.91	8.98	156.31	V. strong
MA7	28.6	53.8	22.83	44.26	1959.11	11.65	0.95	11.03	191.94	V. strong
MA8	26.3	45.3	16.25	38.95	1516.92	10.71	0.89	9.57	166.58	V. strong
MA9	27.8	48.7	11.13	41.52	1723.79	6.46	0.92	5.94	103.33	V. strong
MA10	28.4	45.6	26.68	40.61	1648.90	16.18	0.91	14.73	256.37	E. Strong
MA11	26.8	49.6	19.65	41.14	1692.49	11.61	0.92	10.63	185.04	V. strong
MA12	28.9	45.02	21.75	40.70	1656.58	13.13	0.91	11.97	208.25	V. strong
MA13	28.3	49.8	12.45	42.36	1794.43	6.94	0.93	6.44	112.04	V. strong
UA1	27.6	45.4	25.77	39.94	1595.42	16.15	0.90	14.60	254.04	E. Strong
UA2	28.4	47.7	25.27	41.53	1724.83	14.65	0.92	13.48	234.50	V. strong

V. strong = Very strong E. strong = Extremely strong.

Table 6. Result of slake durability index test of sandstones for two cycles.

SN	Initial weight (gm.)	*IODW* before 1st cycle (gm)	Moisture Content (%)	*ODW* after 1st cycle (gm)	*ODW* after 2nd cycle (gm)	I_{d1}%	I_{d2}%	Durability Classification	Disintegration Type
LA1	531.74	530.61	0.21	529.97	529.34	99.88	99.76	*EH*	I
LA2	507.08	506.81	0.05	504.23	502.6	99.49	99.17	*EH*	I
LA3	534.62	534.59	0.01	533.52	532.77	99.8	99.66	*EH*	I
LA4	513.89	512.95	0.18	511.51	510.59	99.72	99.54	*EH*	I
LA5	512.12	511.96	0.03	510.63	509.66	99.74	99.55	*EH*	I
LA6	532.2	531.72	0.09	530.44	529.11	99.76	99.51	*EH*	I
LA7	548.43	547.68	0.14	545.6	544.34	99.62	99.39	*EH*	I
LA8	529.67	528.8	0.16	526.9	526.26	99.64	99.52	*EH*	I
LA9	516.42	515.09	0.26	513.44	512.41	99.68	99.48	*EH*	I
LA10	546.02	545.72	0.05	544.85	544.14	99.84	99.71	*EH*	I
MA1	541.53	539.84	0.31	539.35	538.65	99.91	99.78	*EH*	I
MA2	549.09	547.53	0.28	543.75	542.99	99.31	99.17	*EH*	I
MA3	530.45	528.56	0.36	525.18	523.96	99.36	99.13	*EH*	I
MA4	519.81	518.14	0.32	517.41	516.64	99.86	99.71	*EH*	I
MA5	549.87	548.37	0.27	544.64	543.82	99.32	99.17	*EH*	I
MA6	543.86	542.01	0.34	540.17	539.35	99.66	99.51	*EH*	I
MA7	540.15	538.2	0.36	535.62	534.38	99.52	99.29	*EH*	I
MA8	540.92	539.61	0.24	538.05	536.16	99.71	99.36	*EH*	I
MA9	546.34	545.69	0.12	541.54	541.27	99.24	99.19	*EH*	I
MA10	511.37	510.87	0.1	509.95	509.34	99.82	99.7	*EH*	I

Table 6. Continued...

SN	Initial weight (gm.)	*IODW* before 1st cycle (gm)	Moisture Content (%)	*ODW* after 1st cycle (gm)	*ODW* after 2nd cycle (gm)	$I_{d1}\%$	$I_{d2}\%$	Durability Classification	Disintegration Type
MA11	521.58	521.11	0.09	519.6	518.87	99.71	99.57	*EH*	I
MA12	538.12	537.13	0.18	535.73	535.04	99.74	99.61	*EH*	I
MA13	491.51	490.31	0.24	487.71	486.73	99.47	99.27	*EH*	I
UA1	499.2	498.59	0.12	497.89	497.24	99.86	99.73	*EH*	I
UA2	513.31	512.59	0.14	511.67	511	99.82	99.69	*EH*	I

Table 7. Water Absorption values of sandstones from the Amile Formation.

S.N.	Dry *wt*.(gm)	Wet. *wt*.(gm)	*WAV%*
LA1	940	940	0
LA2	860	870	1.16
LA3	1500	1500	0
LA4	2910	2920	0.34
LA5	2610	2620	0.38
LA6	2080	2100	0.96
LA7	1080	1090	0.93
LA8	1170	1180	0.85
LA9	1240	1250	0.81
LA10	900	900	0
MA1	750	750	0
MA2	930	940	1.08
MA3	1910	1930	1.05
MA4	1500	1500	0
MA5	690	700	1.45
MA6	1120	1130	0.89
MA7	1270	1280	0.79
MA8	2680	2690	0.37
MA9	460	470	2.17
MA10	1350	1350	0
MA11	1620	1630	0.62
MA12	410	410	0
MA13	1510	1530	1.32
UA1	400	400	0
UA2	840	840	0

Table 8. Correlation between distinct tests under single linear regression.

Correlation	Equation	R^2
PLSI vs SDI	*PLS*I = 11.294*SDI* - 1113	0.8043
PLSI vs WA	*PLSI* = -4.080*WA* + 13.14	0.7982
PLSI vs Pd	*PLSI* = 0.605*Pd* - 45.714	0.8856
PLSI vs Pp	*PLSI* = 0.6233*Pp* - 44.222	0.8353
SDI vs WA	*SDI* = -0.3131*WA* + 99.677	0.7455
SDI vs Pd	*SDI* = 0.0469*Pd* + 95.113	0.8455
SDI vs Pp	*SDI* = 0.0479*Pp* + 95.269	0.7824

This study explored the relationship between *SDI* and the *PLSI* in sandstone samples, revealing a strong correlation with an R^2 of 0.804, significantly higher than the critical r-value (r = 0.337), indicating a meaningful relationship. This finding is consistent with Khajevand & Fereidooni (2018) work, which reported a strong *SDI-PLSI* correlation in travertine samples,

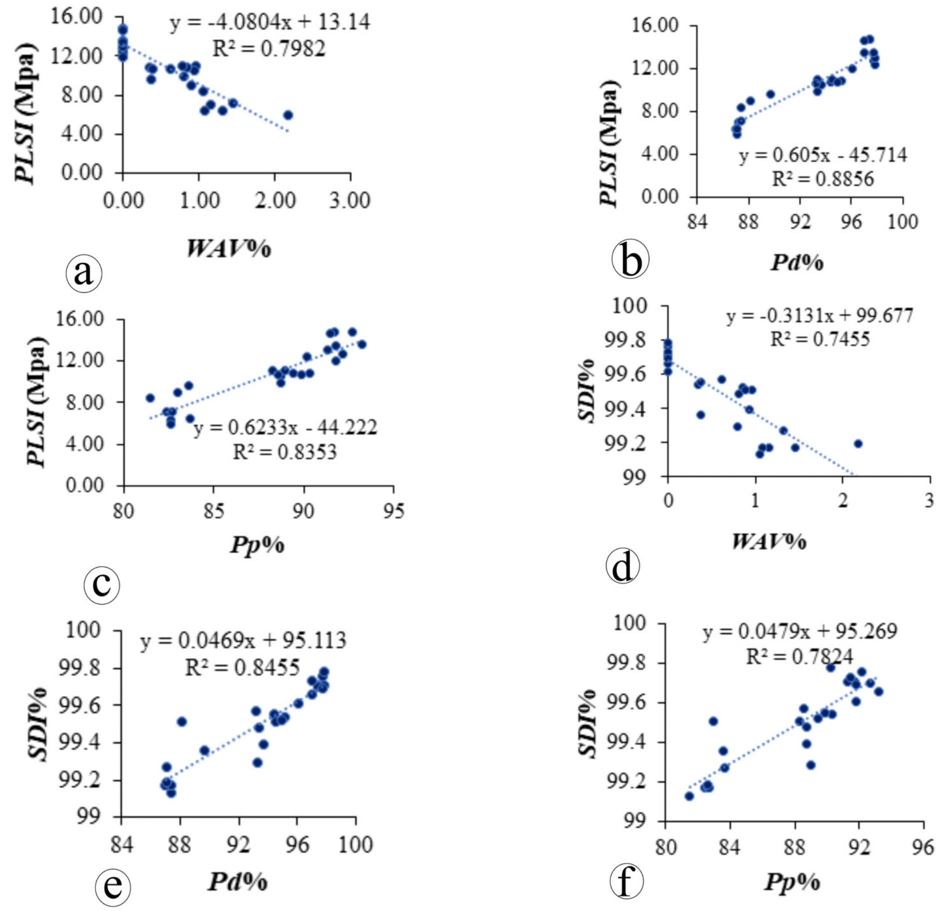

Figure 4. Correlation of best-fitted curve under linear regression (a) *PLSI* vs *WAV* (b) *PLSI* vs *Pd* (c) *PLSI* vs *Pp* (d) *SDI* vs *WAV* (e) *SDI* vs *Pd and* (f) *SDI vs Pp.*

Table 9. Correlation between various tests employing significant independent variables under multiple regression.

Dependent Variable	Independent Variable	Equation	R^2	*SEE*	Critical *r*
SDI	*PLSI*, Water Absorption, Packing density	*SDI* = 96.486 + 0.005*PLSI* - 0.98*WA* + 0.032Pd	0.869	0.082	0.404
SDI	*PLSI*, Water Absorption, Packing proximity	*SDI* = 97.480 + 0.022*PLSI* - 0.109*WA* + 0.02*Pd*	0.848	0.089	0.404
SDI	Water Absorption, Packing proximity	*SDI* = 97.010 -0.153*WA* +0.029*Pp*	0.840	0.892	0.396
SDI	Water Absorption, Packing density	*SDI* = 96.355 -0.105*WA* +0.034*Pd*	0.869	0.080	0.396
PLSI	*SDI*, Water Absorption	*PLSI*= -605.295 +6.204*SDI*-2.138*WA*	0.860	1.051	0.396
PLSI	*SDI*, Water Absorption, Packing density	*PLSI*= -73.998 - 0.48*SDI*-1.470*WA*+0.4064*Pd*	0.916	0.833	0.404
PLSI	*SDI*, Water Absorption, Packing proximity	*PLSI*= -236.624 +2.218*SDI*-1.663*WA*+0.3137*Pp*	0.903	0.894	0.404
PLSI	Packing density, Packing proximity	*PLSI* = -45.584 + 0.662*Pd* - 0.062*Pp*	0.886	0.947	0.396
PLSI	*SDI*, Packing density, Packing proximity	*PLSI* = -285.246 +2.519*SDI* + 0.510*Pd* - 0.025*Pp*	0.892	0.944	0.404
PLSI	*SDI*, Packing density	*PLSI* = -288.944 +2.557*SDI* + 0.485*Pd*	0.892	0.922	0.396
PLSI	*SDI*, Packing proximity	*PLSI* = -530.442 +5.103*SDI* + 0.379*Pp*	0.871	1.007	0.396
PLSI	Water Absorption, Packing density	*PLSI* = -27.794 – 1.52*WA* + 0.423*Pd*	0.916	0.814	0.396
PLSI	Water Absorption, Packing proximity	*PLSI* = -21.409 – 2.002*WA* + 0.378*Pp*	0.898	0.896	0.396

SDI = Slake Durability Index, *PLSI*= Point Load Strength index, *WA*=Water Absorption, *Pd*=Packing density, *Pp*=Packing proximity, *SEE*=Standard error of the estimation and Ahmad et al. (2017), who found an *SDI-PLSI* correlation with an R^2 of 0.812 in sedimentary, metamorphic and igneous rocks altogether 45 samples. However, it contrasts with Liang et al. (2015), who noted a weaker correlation between *SDI* and uniaxial compressive strength (*UCS*) in stronger rocks.

A good correlation was found between *PLSI* vs *WAV* (R^2 = 0.79), *PLSI* vs *Pd* (R^2= 0.88), *PLSI* vs *Pp* (R^2= 0.83), *SDI* vs *WAV* (R^2= 0.74), *SDI* vs *Pd* (R^2= 0.84) and *SDI* vs *Pp* (R^2= 0.78). These results align with Yusof & Zabidi (2016) findings, where higher quartz content and Pd were linked to greater rock strength. The strong correlations observed suggest that *PLSI*, *SDI*, and other physical properties are interconnected and contribute to the mechanical behavior of sandstone from the Amile Formation. These relationships could be useful for geotechnical assessments, allowing for the estimation of one property based on another.

Multiple regression analysis further improved predictive models. For *PLSI*, combining *SDI*, *WAV*, and *Pd* increased the R^2 to 0.916, while for *SDI*, including *WAV* and *Pd* raised the R^2 to 0.869. These findings, consistent with Yusof & Zabidi (2016), build on previous studies by incorporating multiple parameters, offering a more comprehensive understanding of sandstone properties, which could enhance predictions for geotechnical applications.

6 Conclusion

Sandstone from the Amile Formation exhibited extremely high durability (*SDI* 99.17–99.78%) and very strong to extremely strong compressive strength (*PLSI* 5.94–14.81 MPa). The water absorption test results of sandstone from the Amile Formation indicate very low porosity and high resistance to water penetration (*WAV*: 0–2.17%). Based on the strong correlation between *SDI* and *PLSI* (R^2=0.804), future research can use the equation $SDI = 0.0712 PLSI + 98.727$ to estimate *SDI* from *PLSI* for similar sandstones. *PLSI* is well explained by *WAV, Pd*, and *Pp*, whereas *SDI* is explained well by *Pd* and *Pp*. Multiple regression analysis, with an R^2 of 0.869, indicates that *SDI* can be very well explained by *PLSI* in combination with water absorption and *Pd*. Expanding the dataset could improve the study's accuracy.

Acknowledgements

The authors are thankful to the Central Department of Geology, Tribhuvan University and the Department of Mines and Geology, Lainchaur for providing the necessary laboratory facility for conducting the test.

Declaration of interest

The authors have no conflicts of interest to declare. All co-authors have observed and affirmed the contents of the paper and there is no financial interest to report.

Authors' contributions

Saurav Poudel: M.Sc. Dissertation (conceptualization, methodology, writing - original draft). Dr. Naresh Kazi Tamrakar: Dissertation Advisor (supervision, writing - reviewing, and editing).

Data availability

All data produced or examined in the course of the current study are included in this article.

Declaration of use of generative artificial intelligence

This work was prepared with the assistance of generative artificial intelligence (GenAI) OpenAI's ChatGPT with the aim of enhancing readability and refining language. The entire process of using this tool was supervised, reviewed and when necessary edited by the authors. The authors assume full responsibility for the content of the publication that involved the aid of GenAI.

List of symbols and abbreviations

ASTM	American Society for Testing and Materials
De	Equivalent core diameter for an irregular rock lump
F	Size correction factor
Gn	Grain-to-grain contact
I_{d1}	Slake durability index (first cycle)
I_{d2}	Slake durability index (second cycle)
EH	Extremely High
I_s	Uncorrected Point load strength index, Mpa
$I_{s(50)}$	Corrected point load strength
ISRM	International Society for Rock Mechanics
L	Traverse length
MBT	Main Boundary Thrust
MCT	Main Central Thrust
Nc	Total number of contacts
IODW	Initial oven dry weight
ODW	Oven dry weight
Pd	Packing density
PLSI	Point Load Strength Index
Pp	Packing proximity
Q	Quartz
Qm	Monocrystalline quartz
Qp	Polycrystalline quartz
R^2	Relationship coefficient
RF	Rock fragments
SDI	Slake Durability Index
SEE	Standard Error of Estimate
LA	Lower Amile
MA	Middle Amile
UA	Upper Amile

UCS Uniaxial Compressive Strength
XPL Cross-polarized light

References

Ahmad, M., Ansari, M.K., Sharma, L.K., Singh, R., & Singh, T.N. (2017). Correlation between strength and durability indices of rocks-soft computing approach. *Procedia Engineering*, 191, 458-466.

Ahmed, T., Rehman, S.H.U., Ibupoto, F.A., Abbas, A., Ullah, S., Hussain, A., & Usman, S. (2022). Experimental investigation of durability and strength of sandstone and shale of united mineral coal company sor-range, balochistan. *Journal of Mountain Area Research*, 7, 56-62. http://doi.org/10.53874/jmar.v7i0.143.

Aligholi, S., Lashkaripour, G.R., & Ghafoori, M. (2017). Strength/brittleness classification of igneous intact rocks based on basic physical and dynamic properties. *Rock Mechanics and Rock Engineering*, 50(1), 45-65. http://doi.org/10.1007/s00603-016-1106-x.

ASTM D4644-87 (2001). *Standard Test Method for Slake Durability of Shales and Similar Weak Rocks (Reapproved 1992).* Annual Book of ASTM Standards, West Conshohocken, PA.

ASTM C127 (2011). *Standard Test Method for Density, Relative Density (Specific Gravity), and Absorption of Coarse Aggregate*. ASTM International, West Conshohocken, PA, USA.

ASTM D2216 (2019). *Standard Test Methods for Laboratory Determination of Water (Moisture) Content of Soil and Rock by Mass*. ASTM International, West Conshohocken, PA, USA.

ASTM D5731–02 (2003). *Standard test method for determination of point load strength index of rock*. ASTM International, West Conshohocken, PA, USA.

Ayakwah, G., McLemore, V., Fakhimi, A., Viterbo, V., & Dickens, A. (2009). Effects of weathering and alteration on point load and slake durability indices of questa mine materials, New Mexico. *SME Annual Meeting*, 1-50.

Bell, F., & Culshaw, M. (1998). Petrographic and engineering properties of sandstones from the Sneinton Formation, Nottinghamshire, England. *Quarterly Journal of Engineering Geology*, 31(1), 5-19. http://doi.org/10.1144/GSL.QJEG.1998.031.P1.02.

Bell, F.G. (2007). *Engineering geology* (2nd ed.). Butterworth-Heinemann, Elsevier.

Bell, F.G., & Lindsay, P. (1999). The petrographic and geomechanical properties of some sandstones from the Newspaper Member of the Natal Group near Durban, South Africa. *Engineering Geology*, 53(1), 57-81.

Benavente, D., Pla, C., Cueto, N., Galvañ, S., Martínez-Martínez, J., García-del-Cura, M.A., & Ordóñez, S. (2015). Predicting water permeability in sedimentary rocks from capillary imbibition and pore structure. *Engineering Geology*, 195, 301-311. http://doi.org/10.1016/j.enggeo.2015.06.003.

Bieniawski, Z. (1975). The point-load test in geotechnical practice. *Engineering Geology*, 9(1), 1-11. http://doi.org/10.1016/0013-7952(75)90024-1.

Broch E. & Franklin J. (1972). The point-load strength test. *International Journal of Rock Mechanics and Mining Sciences and Geomechanics Abstracts*, 9(6), 669-679. https://doi.org/10.1016/0148-9062(72)90030-7.

Brown, E.T. (1981). *Rock characterization, testing, and monitoring: ISRM suggested methods* (pp. 171-183). Pergamon.

Budhathoki, A., & Tamrakar, N.K. (2022). Durability of sandstones from Sub-Himalaya of central Nepal. *Journal of Nepal Geological Society*, 63, 13-24. http://doi.org/10.3126/jngs.v63i01.50823.

Celik, M.Y., & Kacmaz, A.U. (2016). The investigation of static and dynamic capillary by water absorption in porous building stones under normal and salty water conditions. *Environmental Earth Sciences*, 75(4), 1-19. http://doi.org/10.1007/s12665-015-5132-x.

Cicek, F., Deniz, İ.T., Uck, E., & Kandemir, S.Y. (2016). Determination of Slake Durability Index (Sdi) Values on Different Shape of Laminated Marl Samples. *IOP Conference Series: Earth and Environmental Science*, 44(2), 022006. https://doi.org/10.1088/1755-1315/44/2/022006.

Dhakal, G., Yoneda, T., Kato, M., & Kaneko, K. (2002). Slake durability and mineralogical properties of some pyroclastic and sedimentary rocks. *Engineering Geology*, 65(1), 31-45. http://doi.org/10.1016/S0013-7952(01)00101-6.

Franklin J. A. & Chandra R. (1972). The slake-durability test. *International Journal of Rock Mechanics and Mining Sciences and Geomechanics Abstracts*, 9(3), 325-328. https://doi.org/10.1016/0148-9062(72)90001-0.

Gamble, J.C. (1971). *Durability-plasticity classification of shales and other argillaceous rocks* [Ph.D. thesis]. University of Illinois, Urbana.

Gokceoglu, C., Ulusay, R., & Sönmez, H. (2000). Factors affecting the durability of selected weak and clay-bearing rocks from Turkey, with particular emphasis on the influence of the number of drying and wetting cycles. *Engineering Geology*, 57(3-4), 215-237. http://doi.org/10.1016/S0013-7952(00)00031-4.

Hatheway, A.W. (2009). The complete ISRM suggested methods for rock characterization, testing and monitoring; 1974-2006. *Environmental & Engineering GeoScience*, 15(1), 47-48. https://doi.org/10.2113/gseegeosci.15.1.47.

ISRM. (1981). *Rock characterization testing and monitoring*. Oxford: Pergamon Press.

ISRM. (1985). Suggested method for determining point load strength. *International Journal of Rock Mechanics and Mining Sciences & Geomechanics Abstracts*, 22(2), 51-60.

Kahn, J.S. (1956). The analysis and distribution of the properties of packing in sand-size sediments. On the measurement of packing in sandstone. *The Journal of Geology*, 64, 385-395.

Khajevand, R., & Fereidooni, D. (2018). Assessing the empirical correlations between engineering properties and P wave velocity of some sedimentary rock samples from Damghan, northern Iran. *Arabian Journal of Geosciences*, 11(18), 1-17. http://doi.org/10.1007/s12517-018-3810-1.

Liang, M., Mohamad, E.T., Khun, M.C., & Alel, M.N.A. (2015). Estimating uniaxial compressive strength of tropically weathered sedimentary rock using indirect test. *Jurnal Teknologi*, 72(3), 49-58.

Sabatakakis, N., Koukis, G., Tsiambaos, G., & Papanakli, S. (2008). Index properties and strength variation controlled by microstructure for sedimentary rocks. *Engineering Geology*, 97(1-2), 80-90. http://doi.org/10.1016/j.enggeo.2007.12.004.

Sakai, H. (1983). Geology of the Tansen group of the Lesser Himalaya in Nepal. *Journal of Nepal Geological Society*, 63, 13-24.

Shakoor, A., & Bonelli, R.E. (1991). Relationship between petrographic characteristics, engineering index properties, and mechanical properties of selected sandstones. *Bulletin of the Association of Engineering Geologists*, 28(1), 55-71. http://doi.org/10.2113/gseegeosci.xxviii.1.55.

Sharma, D.R., & Tamrakar, N.K. (2023). Strength and durability status of the Fagfog Quarzite from the Lower Nawakot Group, central Nepal Lesser Himalaya. *Journal of Nepal Geological Society*, 65, 71-88. http://doi.org/10.3126/jngs.v65i01.57753.

Tamrakar, N.K., Yokota, S., & Shrestha, S.D. (2007). Relationships among mechanical, physical and petrographic properties of Siwalik sandstones, Central Nepal Sub-Himalayas. *Engineering Geology*, 90(3-4), 105-123. http://doi.org/10.1016/j.enggeo.2006.10.005.

Tsiambaos, G., & Sabatakakis, N. (2004). Considerations on strength of intact sedimentary rocks. *Engineering Geology*, 72(3-4), 261-273. http://doi.org/10.1016/j.enggeo.2003.10.001.

Tugrul, A., & Zarif, I.H. (1998). The influence of mineralogical textural and chemical characteristics on the durability of selected sandstones in Istanbul, Turkey. *Bulletin of Engineering Geology and the Environment*, 57(2), 185-190. http://doi.org/10.1007/s100640050034.

Vallejo, L.E., Welsh Junior, R.A., & Robinson, M.K. (1989). Correlation between unconfined compressive and point load strengths for Appalachian rocks. In *ARMA US Rock Mechanics/Geomechanics Symposium* (pp. ARMA-89). ARMA.

Yasir, S., Awang, H., & Ayub, M. (2018). The relationship of sandstone's strength with mineral content and petrographic characteristics in Sungai Tekai, Jerantut, Pahang. *AIP Conference Proceedings*, 020010. http://doi.org/10.1063/1.5062636.

Yusof, N., & Zabidi, H. (2016). Correlation of mineralogical and textural characteristics with engineering properties of granitic rock from Hulu Langat, Selangor. *Procedia Chemistry*, 19, 975-980. http://doi.org/10.1016/j.proche.2016.03.144.